# Modal Properties of Child Safety Seats

**J. Giacomin**

Department of Mechanical Engineering, The University of Sheffield
Mappin Street, Sheffield S1 3JD, United Kingdom

This paper describes an experimental modal analysis performed on two stage-1 child safety seats. The objective was to identify whether normal production child seats have frame resonances within the range of human sensitivity to whole-body vibration, and to investigate the nature of the resonances. The results showed that the first mode of vibration of both seats was a torsion mode, which for one seat was at a frequency as low as 17 Hz in one of the test configurations. A frequency of 17 Hz is at the boundary of the region of greatest human sensitivity to vibration in the vertical direction, thus a child would be expected to be quite sensitive at this frequency. Both child seats were found to be highly damped (as much as 10% critical) thus vibrational improvements would probably need to come from changes in mass and stiffness properties. The handle was found to play an important role in determining the vibrational behaviour of the child seat system, with the position greatly affecting the vibrational behaviour. By evaluating the behaviour of the child seat in isolation, this study provides information for the vibrational modelling of the complete system composed of child, child seat and automobile seat.

## Introduction

Numerous studies have investigated the health [8,12,13,16,21,23,25,29] effects of mechanical vibration. National and international standards have been drafted which define the mechanical behaviour of the human body when subjected to vibration [12], and which define weighting filters to estimate subjective comfort [4,8,12]. Numerous studies have also investigated the vibrational comfort of vehicular seats [3,5,7,12,14,28] and test methods have been proposed for their evaluation [10].

A new area of interest is that of the vibrational characteristics of child safety seats [11]. These systems have already benefited from numerous investigations which have evaluated crash safety issues [1,6,17,24,27], but postural, vibrational and other comfort issues are just now being addressed. Comfort is a concern because research to date suggests that small children have well developed sensory capabilities, similar to those of adults [15,26].

This paper describes the results of an experimental modal analysis performed on two stage-1 child safety seats (children less than 10 kg and 9 months of age). The objective was to identify whether normal production child seats have frame resonances within the range of human sensitivity to whole-body vibration from .05 to 100 Hz, and to investigate the nature of the resonances. Analysing the behaviour of the seats in isolation was necessary in order to identify the contribution of the child seat frame to the global dynamic behaviour of the system composed of automobile seat, child seat and child. If the whole-body frequency weighting curves of BS 6841 [4] which were determined using adult subjects can be applied in the case of small children, then it would seem appropriate that a child seat have a first frame resonance as far above 16 Hz as possible. This is because 16 Hz represents the upper limit of the region of greatest human sensitivity to whole-body vibration in the vertical direction as defined by the asymptotic approximation to filter $W_b$ [4].

The modal analysis was performed using two different positions for the handle, the handle-down position which is the normal operating position when travelling in the vehicle and the handle-up position which can be used otherwise. By performing the tests in the two positions it was expected that an overview of the influence of the handle on the dynamics of the complete child seat would be obtained.

**Test Rig**

A small rig was built to test the child seats, which is presented in Figure 1 below.

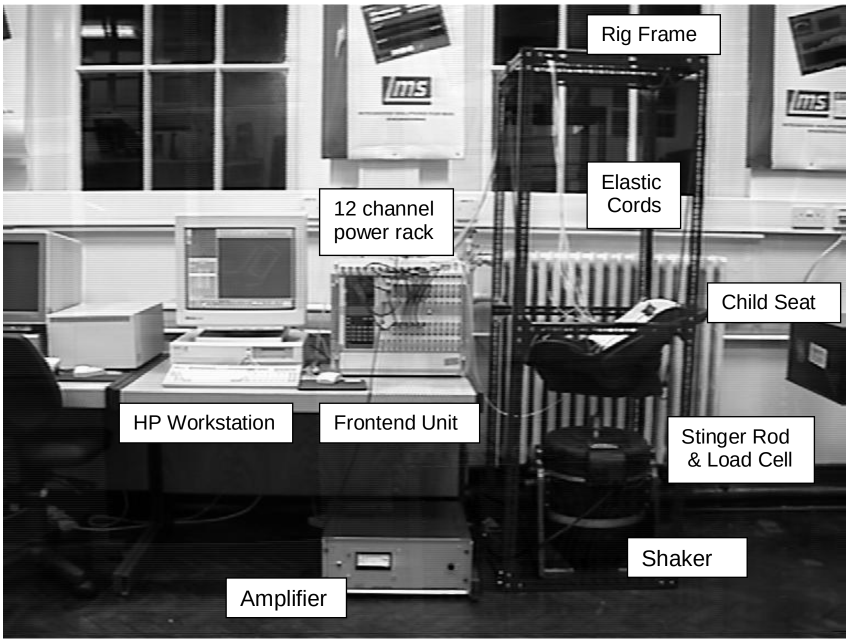


Figure 1) Child seat test rig.

The rig consisted of a support frame which suspended the child seat by means of elastic cords. The frame was centred over a model 501 electrodynamic shaker manufactured by Ling Dynamics Ltd. [18]. The shaker is designed for operation in the frequency range from 1.5 to 3000 Hz. The maximum force rating is 908 N, and the maximum rated bare table acceleration is 40 g.

The child seat was connected to the shaker by means of a stinger-rod [9,22] which excited the child seat from below in the vertical direction. The point of attachment was chosen so as to be forward and to the left of the centre of gravity of the seat. This placement of the vibration input location avoided the symmetry planes of the seat and thus guaranteed that both bending and torsion modes would be excited simultaneously. A PCB model 208B01 force transducer was mounted on the seat end of the stinger rod to measure the input force. The transducer had a sensitivity of 122.1 mv/N and a linear operating range from 0 to 90 Newtons. The frequency range of the load cell extends from about 1 Hz (depending on the force amplitude) to more than 50 kHz.

The signal generation and data analysis was performed using an LMS CADA-X revision 3.4 software system. The software was run on an HP model 715/64 workstation and a Difa Measuring

Systems SCADAS II front-end was used. Test signal generation and data acquisition were performed using the Fourier Monitor [FMON] module of the CADA-X system [19]. Mode shape vectors and loss factors were calculated in the MODAL ANALYSIS module [20]. The tests were performed using a band-limited random force signal in the frequency range from 1 to 100 Hz which produced acceleration levels on the seat frame which were similar to those measured during in-vehicle tests [11]. The RMS input force level was 6.6 N in the case of Seat-A and 4 N in the case of Seat-B. The average output RMS acceleration level at point 2 of Seat-A in the vertical direction was .75 $m/s^2$ while it was .37 $m/s^2$ for Seat-B.

**The Child Seats**

Two seats were chosen. Seat-A had a stiff frame which would be expected to produce a relatively high value for the system first natural frequency. The frame of Seat-A was a standard component shared by seats produced by several different manufacturers, so the results can be considered representative of a range of currently available products. Seat-A was also a useful test specimen because the handle folded down into a resting position against the frame when in use in the vehicle. This stow-away position greatly diminished the effect of the handle on the dynamics of the complete seat.

Seat-B was a very different design which used a much softer plastic material for the frame, which was expected to lead to a relatively low first natural frequency. Seat-B was representative of a class of seats in which the handle remains extended during use so as to support the child seat against the automobile seat cushion. The overhanging handle was expected to contribute greatly to the overall dynamics. The two seats are shown in Figure 2 below.

Seat-A Seat-B

Figure 2) Stage-1 child safety seats tested.

**Measurement Points and Child Seat Geometry Model**

Twelve accelerometers were attached to each frame in such a way as to provide a reasonably clear representation of the first torsional and the first bending mode shape vector. Figure 3 presents the accelerometer layout established for Seat-A. The vertical direction of the child seat and the automobile is given as Z, the for-aft direction is labelled X and the lateral direction is labelled as Y.

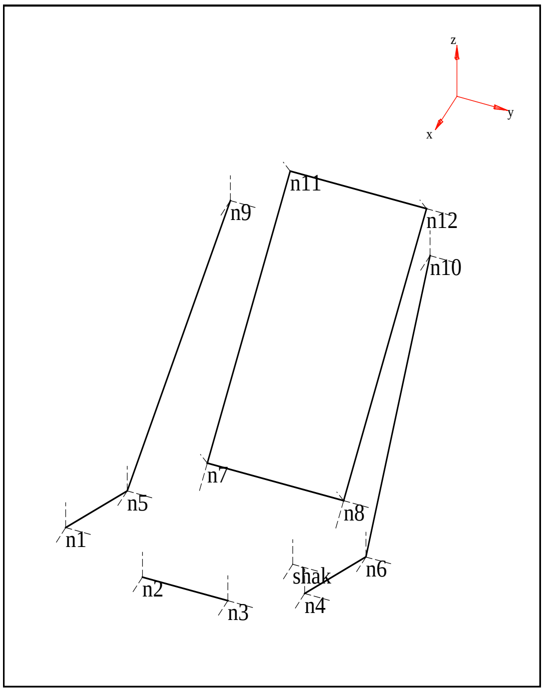


Figure 3) Geometry model for Seat-A.

Six accelerometers were placed along the inner surface, with the measurement axis pointing in the direction normal to the surface. These accelerometers were labelled n2, n3, n7, n8, n11 and n12. The accelerometers at positions n2 and n3 pointed almost directly in the vertical direction Z, while those at n7, n8, n11 and n12 pointed normal to the backrest section of the child seat which made an angle of 120 degrees with respect to X axis of the seat (i.e. reclined back at 30 degrees with respect to the vertical). A further 6 accelerometers (numbered n1, n4, n5, n6, n9 and n10) were placed along the sides of the frame pointing normal to these surfaces, thus measuring vibration in the lateral direction Y.

When viewing the geometry model or interpreting the mode shape vectors, it is important that the reader recall that only single-axis accelerometers were used. Only one translational movement was measured at each node point rather that the full set of three possible translations. Only translations in the lateral (Y) direction were measured for nodes n1, n4, n5, n6, n9 and n10 while only vertical (Z) translations were measured for nodes n2 and n3. Nodes n7, n8, n11 and n12 measured translations along an axis in the X-Z plane.

## Identification From Experimental Data

The experimental modal analysis was performed using the LMS Modal Analysis package [20]. The method selected for use was the Frequency Domain Direct Parameter Identification method (FDPI) which is known to be robust and to work well for highly damped systems. The FDPI method estimates the parameters of a spatial system model [22] directly from the measured frequency domain FRFs by assembling a system of equations of the form

$$[M][\ddot{x}(t)] + [C][\dot{x}(t)] + [K][x(t)] = [M][\ddot{z}(t)] + [F(t)]$$

where [M], [C] and [K] are the mass, stiffness and damping matrices for the system of oscillators, [F] is a vector of external forces acting on the individual masses and [Z] is a vector of base excitation movements acting on the masses indirectly through springs and dampers. By assuming harmonic excitation and performing some algebraic manipulation, the matrix equation for a system with $N_i$ inputs and $N_o$ outputs can be written in the frequency domain as

$$\left[\omega^2[I] + j\omega[A_1] + [A_0]\right][H(\omega)] = j\omega[B_1] + [B_0]$$

where: $[A_1] = [M]^{-1}[C]$ is the mass modified damping matrix of order $N_0$ by $N_o$

$[A_0] = [M]^{-1}[K]$ is the mass modified stiffness matrix of order $N_0$ by $N_o$

$[H(\omega)]$ is the matrix of FRFs of order $N_o$ by $N_I$

$[B_0]$ and $[B_1]$ are the force distribution matrices of order $N_o$ by $N_I$

The matrix equation above provides a format for estimating the constant coefficients of the matrices $[A_1]$, $[A_0]$, $[B_1]$ and $[B_0]$ which are solved by means of regression analysis. Once the $[A_1]$, $[A_0]$, $[B_0]$ and $[B_1]$ matrices are estimated by regression analysis, the natural frequencies and mode shape vectors can be calculated by standard methods [9,22].

## Results

Figure 4 presents the accelerance and coherence functions [9,22] from the input point to measurement point n2 in the frequency range from 1 to 100 Hz. The figure presents the results for both Seat-A and Seat-B in the handle down position (the in-vehicle position). The modulus curves show a number of resonances below 7 Hz which are not discussed further in this paper. These resonances were checked numerically and by visual inspection and were found to be rigid body modes of the seat oscillating on the stinger rod.

Both seats had resonances in the range of interest of human whole-body vibration from .05 to 100 Hz. The accelerance modulus curves of Figure 4 show resonances for Seat-A at about 35, 73 and 92 Hz while the modulus curves for Seat-B show resonances at 17, 19, 26, 29, and 71 Hz.

Additional resonance frequencies are more clearly visible on the accelerance functions for other measurement points such as n9. All accelerance functions showed broad peaks, indicating high levels of damping. The half power points often covered a frequency span of from 2 to 5 Hz in width, which at the higher frequencies meant damping values of as much as 10% of critical.

Seat-B was found to have more resonance frequencies in the range of interest for whole-body vibration. More importantly, Seat-B was found to have a low first natural frequency of 17 Hz. This result is important because it is almost within the frequency range of greatest sensitivity to vibration (5-16 Hz for adults) which suggests that the child seat frame could amplify human discomfort.

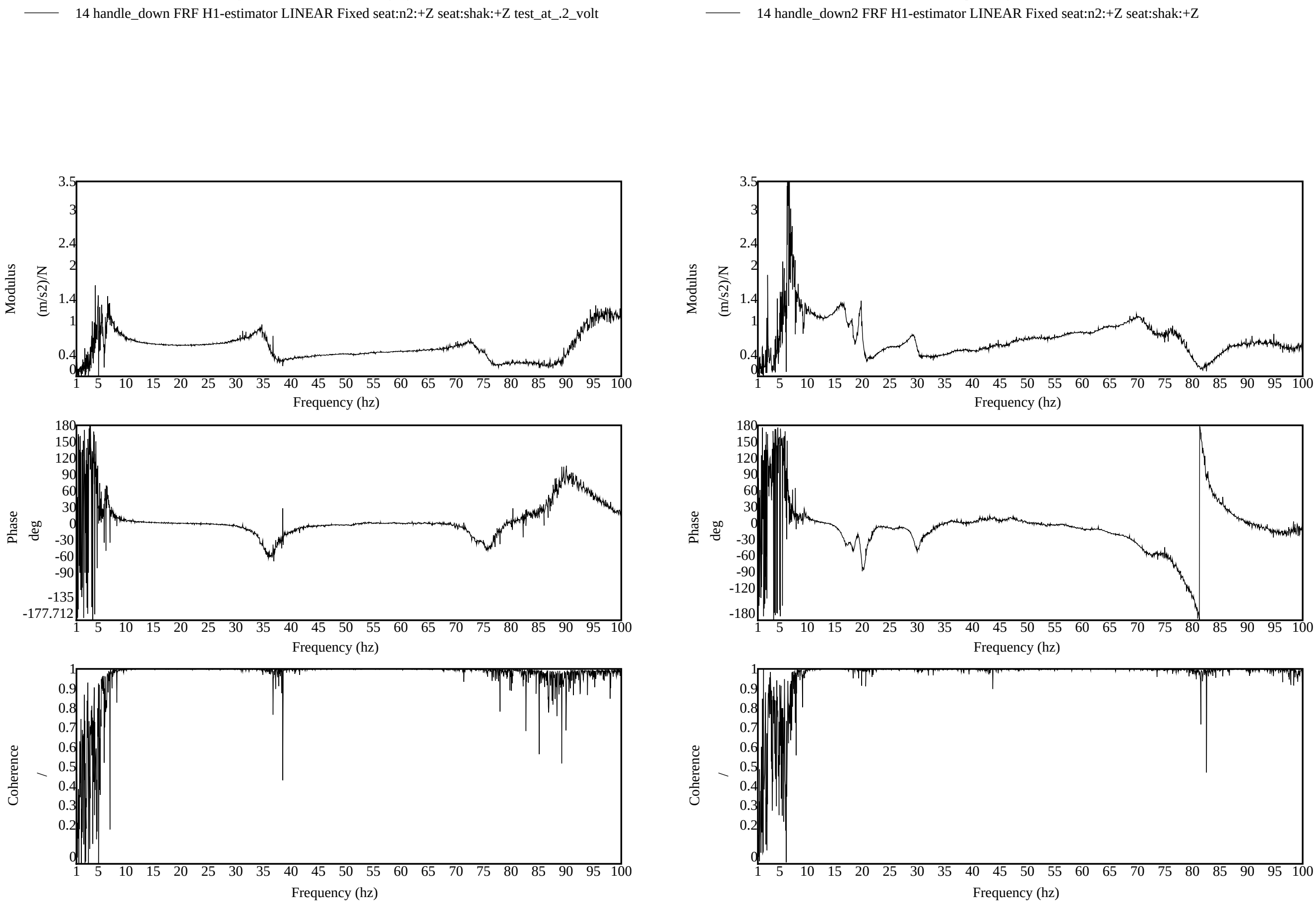


Seat-A in handle-down position

Seat-B in handle-down position

Figure 4) Accelerance and coherence functions from input to point n2 for seats A and B.

Figure 5 compares the accelerance functions from the force input location to point n9 for Seat-A in the handle-down and in the handle-up position. It can be seen that there are significant differences between the accelerance functions obtained in the two positions. Among the differences, it can be seen that the handle-up FRFs were always “noisier” than those with the handle down for the same number of averages. The “noise” in the FRFs might be explained by impacts occurring at the handle hinges where there was free play. Occasional impact phenomena caused by the flapping handle hitting the frame would modify the energy flow across the structure and thus effect the FRFs. This hypothesis can be supported by the lower coherency values at many frequencies.

For Seat-A the handle-up results showed that new resonance frequencies (at 20 and 48 Hz) were present with respect to the handle-down position. These resonance frequencies were *in addition* to those previously measured in the handle-down position and were due to the dynamics of the handle.

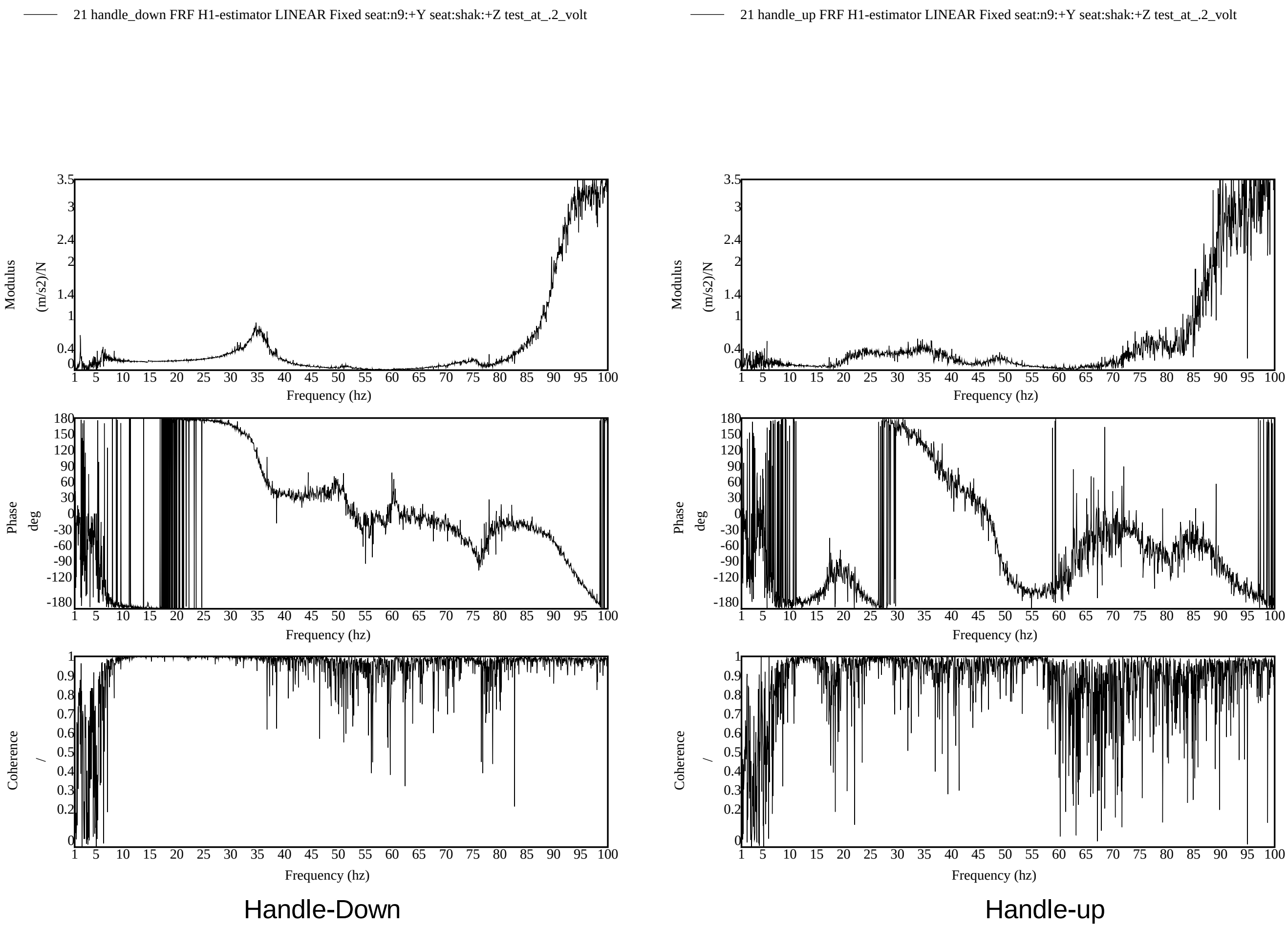


Figure 5) Accelerance and coherence functions from input to point n9 for Seat-A.

Figure 6 presents the three mode shape vectors for Seat-A in the handle-down position. All three mode shape vectors are illustrated using the same scale factor so that the amplitudes can be compared. From Figure 6 it can be seen that the first mode of vibration is a torsional mode. The child seat shell, while complicated in it's details, resembles an elongated open U-section with a bend in the middle. The test results showed that both seats were weak in torsion as is typical of open sectioned beams.

The second mode shape vector of Seat-A showed lateral bending which produced the highest frame movements at the centre near the handle mounting points. The small amplitude of frame vibration associated with this mode (compared to the first or third) suggests that it was mainly handle movement. The third mode of vibration produced again large amplitudes, and was principally an in-and-out flapping movement of the frame side panels.

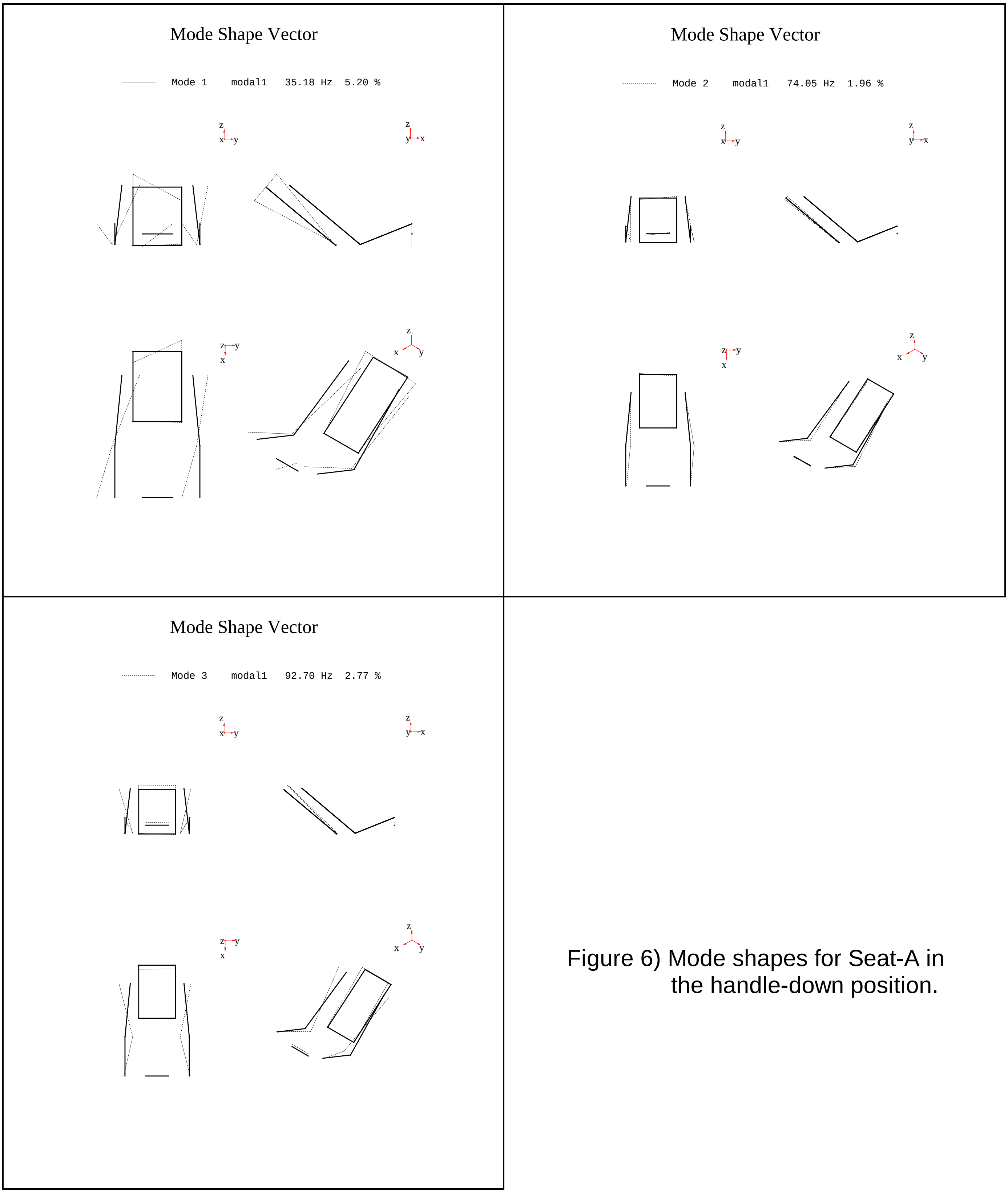


Figure 6) Mode shapes for Seat-A in the handle-down position.

Tables 1, 2, 3 and 4 summarise the results from all the modal analysis tests performed. A short verbal description of the mode shape is given where possible, question marks indicate the resonances for which a clear understanding was not possible because of problems such as spatial aliasing [9,22].

| Mode Number | Frequency (Hz) | Modal damping (%) | Shape |
|---|---|---|---|
| 1 | 35.18 | 5.2 | Frame first torsion mode |
| 2 | 74.05 | 1.96 | Frame lateral bending |
| 3 | 92.70 | 2.77 | Frame side flapping |

Table 1) Vibrational modes up to 100 Hz for Seat-A in the handle-down position.

| Mode Number | Frequency (Hz) | Modal damping (%) | Shape |
|---|---|---|---|
| 1 | 20.46 | 6.93 | Handle mode |
| 2 | 35.88 | 7.29 | Frame first torsion mode |
| 3 | 48.61 | 3.38 | Handle mode |
| 4 | 75.17 | 3.24 | Frame lateral bending |
| 5 | 90.56 | 1.85 | Frame side flapping |

Table 2) Vibrational modes up to 100 Hz for Seat-A in the handle-up position.

| Mode Number | Frequency (Hz) | Modal damping (%) | Shape |
|---|---|---|---|
| 1 | 17.05 | 7.29 | Frame first torsion mode |
| 2 | 19.84 | 7.13 | Handle mode with frame torsion |
| 3 | 26.32 | 9.86 | Handle mode with frame torsion |
| 4 | 29.52 | 3.02 | Front frame twisting and handle |
| 5 | 42.89 | 6.53 | Side wings flapping |
| 6 | 71.79 | 6.98 | ? |
| 7 | 83.40 | 3.94 | ? |
| 8 | 97.24 | 4.99 | ? |

Table 3) Vibrational modes up to 100 Hz for Seat-B in the handle-down position.

| Mode Number | Frequency (Hz) | Modal damping (%) | Shape |
|---|---|---|---|
| 1 | 20.81 | 3.86 | Frame first torsion mode |
| 2 | 24.37 | 3.98 | Handle mode with frame torsion |
| 3 | 30.38 | 4.76 | Frame twisting with handle |
| 4 | 41.85 | 6.62 | Side wings flapping |
| 5 | 44.90 | 1.72 | ? |
| 6 | 78.55 | 3.82 | ? |
| 7 | 95.66 | 5.04 | ? |

Table 4) Vibrational modes up to 100 Hz for Seat-B in the handle-up position.

## Discussion

An important result was that Seat-B had a frame flexible body resonance at 17 Hz which is almost in the range of maximum human sensitivity to vertical whole-body vibration. Such a frame resonance will amplify human discomfort if there is significant energy present in the road input to the vehicle. The asymptotic approximations of the frequency weighting filters of BS 6841 give a weighting value of 1.0 (the maximum) for the frequency range from 5 to 16 Hz and a value of 16/f for the frequencies from 16 to 80 Hz. At 17 Hz this gives a weighting value of .94 which is high, and thus important to human perception. Seat-A had a first resonance frequency of 35 Hz and is thus better suited to isolating the child from road vibrations since the BS 6841 filter value at 35 Hz is .45, less than half.

Another observation is that the first mode of vibration for both child seats is a torsional mode, which is logical considering the open U-section shape of the frame. The natural frequency of the first resonance could perhaps be increased by stiffening the child seat with cross-ribbing under the lower surface along the lines of torsional strain.

Both seats had resonance frequencies in the range of human perception of whole-body vibration (.05-100 Hz). Seat-A had 3 in the handle-down position and 5 in the handle-up position, while Seat-B had 8 in the handle-down position and 7 in the handle-up position. The presence of these frame resonances means that the vibration at the interface between the automobile seat and the child safety seat will often be amplified at frequencies that are important to human comfort. Unless child safety seat frames become stiffer in the future, it will be necessary to include the flexible body dynamics of the child seat frame in vibrational models of the system composed of the child, the child seat and the automobile seat.

Damping levels were found to be high for both seats, with Seat-B providing higher levels of damping than Seat-A. The test results suggest that damping treatments may not be the best way to improve the vibrational behavior of the seat frames. The frame plastic and the trim foam have already achieved a very useful level of damping (as much as 10% critical) in the two seats tested, the levels were as high as what is normally achieved in practice using constrained layer damping treatments [2]. The results suggest that it may be more useful to seek further vibration reduction by means of mass and stiffness modification.

Another useful finding was the importance of the handle towards the seat dynamics. The results suggest that stowing the handle against the frame rather than leaving it exposed during travel can simplify the dynamics of the child seat system thus making it easier for the designer to optimise the vibrational behavior of the complete system.

In the coming months measurements will be performed of the apparent mass of several small children and a model of the complete system composed of the child, child seat and automobile seat will be established.

## References


[1] Bell, R., Burleigh, D. and Czernakowski, W. 1994, ISOFIX: The potential of a universal vehicle/child restraint interface for misuse reduction and performance enhancement, SAE paper 942220

[2] Beranek, L.L. and Ver, I.L. 1992, Noise and vibration control engineering, John Wiley & Sons Inc., New York

[3] Berger, E. and Gilmore, B.J. 1993, Seat dynamic parameters for ride quality, SAE paper 930115

[4] British Standards Institution 1987, Measurement and evaluation of human exposure to whole-body vibration and repeated shock, BS 6841

[5] Brite Euram Project 5549 Advanced Technologies for Automotive Seat Evaluation and Design 1995, 30 Month progress report for the European Commission, Contract BRE2-CT92-0246 (SED)

[6] Carlsson, G., Norin, H. and Ysander, L. 1991, Rearward-facing child seats: the safest car restraint for children ?, Accid. Anal. Prev., Vol. 23, No. 2-3, pp 175-182

[7] Corbridge, C., Griffin, M.J. and Harborough, P.R. 1989, Seat dynamics and passenger comfort, Proc. Instn. Mech. Engrs., Vol. 203, pp 57-64

[8] Dupius, H. and Zerlett, G. 1986, The effects of whole-body vibration, Springer-Verlag, Berlin

[9] Ewins, D.J. 1984, Modal Testing: Theory and Practice, Research Studies Press Ltd., Taunton, Somerset

[10] Giacomin, J. and Bracco, R. 1995, An experimental approach for the vibration optimisation of automotive seats, ATA 3rd Int. Conf. on Vehicle Comfort and Ergonomics, Bologna, Italy, March 29-31, pp 199-208
[11] Giacomin, J. 1996, Vibration characteristics of child safety seats, Conference Metodologie per l'Ergonomia, Torino, Italy, 21 November
[12] Griffin, M.J. 1990, Handbook of human vibration, Academic Press, London
[13] Ishihara, H., Tsuji, H., Hirano, N., Ohshima, H. and Terahata, N. 1992, Effects of continuous quantitative vibration on rheologic and biological behaviors of the intervertebral disc, Spine, Vol. 17, No. 3S, pp s7-s12
[14] Joyce, J. and Dunn, W.H. 1992, Evaluation of seat design parameters for improved occupant ride, IMechE paper 925172
[15] Kaufmann, F. 1995, Development of motion perception in early infancy, European Journal of Pediatrics, Vol. 154, No. 9, S4, s48-s53
[16] Kelsey, J.L. 1975, An epidemiological study of the relationship between occupations and acute herniated lumbar intervertebral discs, Int. Journal of Epidemiology, Vol. 4, No.3, pp 197-205
[17] Kuhane, C.J. 1986, An evaluation of child passenger safety: the effectiveness and benefits of safety seats, DOT-HS-806-890, National Highway Traffic Safety Administration, Washington D.C.
[18] Ling Dynamic Systems Ltd 1977, Vibrator Model 501 Instruction Manual, Ling Dynamics Systems Ltd, Royston, Hertfordshire
[19] LMS International 1996, LMS CADA-X Fourier Monitor Manual, Revision 3.4, LMS International, Leuvan
[20] LMS International 1996, LMS CADA-X Modal Analysis Manual, Revision 3.4, LMS International, Leuvan
[21] McLain, R.F. and Weinstein, J.N. 1994, Effects of whole body vibration on dorsal root ganglion neurons, Spine, Vol. 19, No. 13, pp 1455-1461
[22] Maia, N.M.M. and Montalvao e Silva, J.M. 1997, Theoretical and experimental modal analysis, Research Studies Press Ltd., Taunton, Somerset
[23] Necking, L.E., Dahlin, L.B., Friden, J., Lundborg, G., Lundstrom, R. and Thornell, L.E. 1992, Vibration induced muscle injury, The Journal of Hand Surgery, Vol. 17B, No. 3, June, pp 270-274
[24] Pedder, J., Legault, F., Salcudean, G., Hillebrandt, D., Gardner, W. and Labrecque, M. 1994, Development of the CANFIX infant and child restraint/vehicle interface system, SAE paper 942221
[25] Pope, M.H. and Hansson, T. 1992, Vibration of the spine and low back pain, Clinical Orthopaedics and Related Research, No. 279, June, pp 49-59
[26] Roessler, J.S. and Dannemiller, J.L. 1997, Changes in human infants' sensitivity to slow displacements over the first 6 months, Vision Res., Vol. 37, No. 4, pp 417-423
[27] Ruta, D., Beattie, T. and Narayan, V. 1993, A prospective study of nonfatal childhood road traffic accidents - what can seat restraint achieve, Journal of Public Health Medicine, Vol. 15, No. 1, pp 88-92
[28] Staszewski, W.J. and Giacomin 1997, J., Application of wavelet based FRF's to the analysis of nonstationary vehicle data, 15th Int. Modal analysis Conference, Orlando, Florida, Feb. 3-6
[29] Wilder, D.G., Frymoyer, J.W. and Pope, M.H. 1985, The effect of vibration on the spine of the seated individual, Automedica, Vol. 6, pp 5-35